Journal of Alloys and Compounds, 186 (1992) 321–331
JALCOM 274

Crystal structure and physical properties of the carbides UAl_3C_3 and $YbAl_3C_3$

Thorsten-M. Gesing, Rainer Pöttgen, Wolfgang Jeitschko and Ulrich Wortmann
Anorganisch-Chemisches Institut, Universität Münster, Wilhelm-Klemm-Strasse 8, W-4400 Münster (Germany)

(Received February 15, 1992)

Abstract

UAl_3C_3 – previously described with the tentative composition UAl_5C_4 – was prepared from the elemental components by arc melting. The new compound $YbAl_3C_3$ was obtained best in a lithium flux, which subsequently was dissolved in ethanol. Both carbides are isotypic with $ScAl_3C_3$. Their hexagonal lattice constants are $a = 339.88(5)$ pm, $c = 1711.3(2)$ pm and $a = 338.9(1)$ pm, $c = 1739.4(3)$ pm for the ytterbium and uranium compound respectively. The crystal structure of UAl_3C_3 was refined from single-crystal X-ray data to a residual of $R = 0.039$ for 231 structure factors and 12 variable parameters. Mass spectroscopy analyses of the hydrolyses products of $YbAl_3C_3$ and UAl_3C_3 with 2N hydrochloric acid essentially show only methane. Magnetic susceptibility measurements with a SQUID magnetometer indicate antiferromagnetism with Néel temperatures $T_N = 8 \pm 1$ K ($YbAl_3C_3$) and $T_N = 13 \pm 1$ K (UAl_3C_3). At lower temperatures the uranium compound shows metamagnetic behaviour. Electrical conductivity measurements of a single crystal of $YbAl_3C_3$ indicate semiconductivity.

1. Introduction

While the only binary aluminium carbide Al_4C_3 has been known for a long time [1, 2], ternary carbides containing aluminium were described much later, *e.g.* Cr_2AlC [3], Mo_3Al_2C [4], Sc_3AlC [5], $Mo_{12}Cu_3Al_{11}C_6$ [6], $ZrAlC_2$ [7], $Zr_2Al_3C_5$ [8], Hf_5Al_3C [8] and Ti_3NiAl_2C [9]. With the actinoids ternary carbides were reported with the tentative compositions $Th_4Al_2C_5$, $ThAlC_2$, $ThAl_4C_4$ [10], UAl_5C_4 and $U_2Al_3C_3$ [11]. In the present investigation we have determined the crystal structure of the compound "UAl_5C_4". The correct composition was found to be UAl_3C_3. This carbide is isotypic with $ScAl_3C_3$ [12]. In addition, we report on the preparation of the new carbide $YbAl_3C_3$, which has the same structure, and on the chemical and physical properties of both compounds.

2. Sample preparation and lattice constants

Starting materials were platelets of uranium (Merck, "nuklearrein"), ytterbium filings (Kelpin, 99.9%), aluminium foil (Alpha, 99.9%) and graphite

0925-8388/92/$5.00

flakes (Alpha, 99.5%). The uranium platelets were cleaned with concentrated nitric acid to remove oxide impurities. UAl_3C_3 was prepared by arc melting cold-pressed pellets (about 500 mg) of the elemental components with the ideal composition in an atmosphere of purified argon. To ensure homogeneity, the buttons were turned around and melted again. After the arc-melting process the samples were annealed slightly below the melting point in evacuated, water-cooled silica tubes in a high frequency furnace for about 4 h.

Samples of the ytterbium compound prepared in the same way contained $YbAl_3C_3$ only to about 70%. In well-crystallized pure form this carbide was obtained from a lithium flux. The elements, in the atomic ratio Yb:Al:C:Li = 1:3:3:30, were sealed in iron tubes (tube volume 4 cm^3) in an argon atmosphere. They were annealed at 800 °C for 1 day and subsequently cooled at 7 K h^{-1} to room temperature. After the cooling process the lithium matrix was dissolved in dried ethanol. The resulting small hexagonal platelets of $YbAl_3C_3$ were further purified in ethanol in an ultrasonic bath.

Energy-dispersive X-ray analyses of all samples did not reveal any impurity elements such as silicon or iron. The samples were characterized through their Guinier powder patterns with Cu $K\alpha_1$ radiation. The identification of the diffraction lines was facilitated by intensity calculations [13] using the positional parameters of the refined structure. As an example the evaluation of the $YbAl_3C_3$ diagram is shown in Table 1. The lattice constants were obtained by least-squares fits with α-quartz ($a = 491.30$ pm, $c = 540.46$ pm) as an internal standard. The hexagonal lattice constants of $YbAl_3C_3$ prepared by arc melting ($a = 339.0(2)$ pm, $c = 1713.0(7)$ pm, $V = 0.1705(3)$ nm^3) and by the lithium flux ($a = 339.88(5)$ pm, $c = 1711.3(2)$ pm, $V = 0.1712(2)$ nm^3) were the same within three standard deviations. The lattice constants of UAl_3C_3 are $a = 338.9(1)$ pm, $c = 1739.4(3)$ pm and $V = 0.1730(2)$ nm^3.

3. Properties

Well-crystallized samples of UAl_3C_3 and $YbAl_3C_3$ have a light grey colour with metallic lustre; powdered samples are black. They react readily with the humidity of the air; microcrystalline samples are completely decomposed after a few hours.

Both compounds were hydrolysed in diluted (2N) hydrochloric acid. The gaseous reaction products were analysed in a mass spectrometer (CH5, Varian MAT, 20 °C, 70 eV). UAl_3C_3 gave only CH_4 and the corresponding fragments CH_3, CH_2, CH and C. The sample of $YbAl_3C_3$ gave 95% CH_4 (including the fragments) and at most 5% C_2 hydrocarbons. In view of the UAl_3C_3 result, one may assume that the C_2 hydrocarbons obtained from the $YbAl_3C_3$ sample are due to a minor amount of an impurity phase, *e. g.* YbC_2 or Yb_3C_4 (formerly described as $Yb_{15}C_{19}$ [14, 15]), which are known to develop various C_2 hydrocarbons [16, 17].

The magnetic susceptibilities of the polycrystalline samples (about 2 mg) were determined with a SQUID magnetometer at temperatures between

TABLE 1

Powder pattern of $YbAl_3C_3$[a]

$h\ k\ l$	Q_o	Q_c	I_o	I_c
0 0 2	136	137	vs	100
0 0 4	546	546	m	22
1 0 0	1155	1154	m	16
1 0 1	–	1188	–	<1
0 0 6	1227	1229	w	6
1 0 2	1290	1291	vs	88
1 0 3	1462	1462	vw	2
1 0 4	1700	1701	s	60
1 0 5	2010	2008	w	6
0 0 8	2183	2185	w	14
1 0 6	2384	2384	s	42
1 0 7	–	2828	–	<1
1 0 8	3342	3340	w	10
0 0 10	3414	3415	vw	2
1 1 0	3463	3463	s	27
1 1 2	3600	3599	w	11
1 0 9	3921	3920	vw	1
1 1 4	4008	4009	w	10
1 0 10	4569	4569	m	16
2 0 0	4616	4617	vw	3
2 0 1	–	4651	–	<1
1 1 6	4690	4692	w	6
2 0 2	4757	4754	m	15
0 0 12	4919	4917	vw	2
2 0 3	–	4924	–	<1
2 0 4	5160	5163	m	13

[a] The pattern was recorded in a Guinier camera with Cu $K\alpha_1$ radiation. The Q values are defined by $Q = 100/d^2$ (nm^{-2}). The observed intensities I_o from very weak to very strong are abbreviated by vw, w, m, s and vs.

2 and 300 K with magnetic flux densities between 0.1 and 5 T. The magnetic susceptibility of $YbAl_3C_3$ is independent of the magnetic field. At low temperature an antiferromagnetic minimum is observed in the $1/\chi$ *vs.* T plot (Fig. 1) with a Néel temperature $T_N = 8 \pm 1$ K. At temperature above 150 K the magnetic susceptibility seems to obey the Curie–Weiss law; however, the magnetic moment $\mu_{exp} = 5.3\ \mu_B$ calculated from the slope of this nearly straight line is too high to be attributable to the Yb^{3+} ions (the free-ion value for Yb^{3+} according to $\mu_{eff} = g[J(J+1)]^{1/2}$ is 4.54 μ_B). We conclude that the susceptibility behaviour of this compound reflects the intermediate valent character of the ytterbium ions, as is also indicated by the volume plot for this compound (Fig. 2). A much flatter $1/\chi$ *vs.* T plot was obtained for $YbNi_2P_2$ [18]. There a naive evaluation according to the Curie–Weiss law would have resulted in an almost infinite magnetic moment.

The magnetic behaviour of UAl_3C_3 is more complex. The susceptibility of this compound is slightly field dependent at temperatures above 150 K,

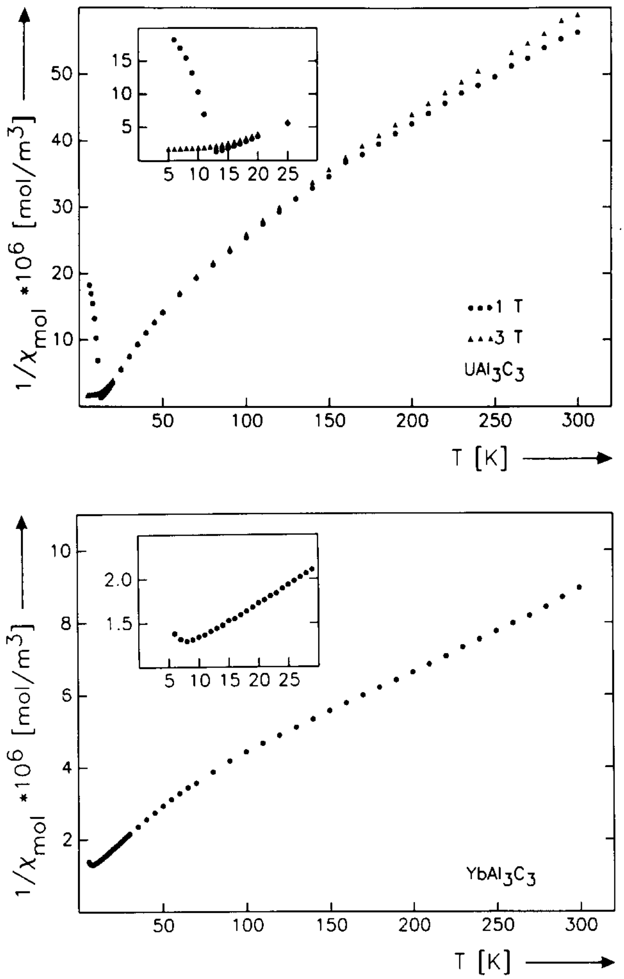

Fig. 1. Reciprocal magnetic susceptibility of UAl_3C_3 and $YbAl_3C_3$ as a function of temperature. The insets show the reciprocal susceptibilities at low temperatures. The susceptibilities of the uranium compound were measured in magnetic fields of 1 and 3 T; the susceptibility of the ytterbium compound is independent of the field strength.

probably owing to a very small amount of a ferromagnetic impurity. In this temperature range the susceptibility nearly obeys the Curie–Weiss law. At low temperatures UAl_3C_3 orders antiferromagnetically with a Néel temperature $T_N = 13 \pm 1$ K (Fig. 1). A least-squares fit of the data above 30 K according to the formula $\chi = \chi_0 + C/(T - \Theta_W)$ resulted in a Weiss temperature $\Theta_W = -9 \pm 1)$/K and an effective magnetic moment $\mu_{exp} = (8C)^{1/2} = 1.52 \pm 0.05\ \mu_B$. This value is much smaller than the free-ion value for U^{3+}, $\mu_{eff} = 3.63\ \mu_B$, thus indicating a low degree of 5f electron localization in our compound. At low temperatures the magnetic susceptibility of UAl_3C_3 became field dependent, in a way suggesting metamagnetic behaviour. This was confirmed

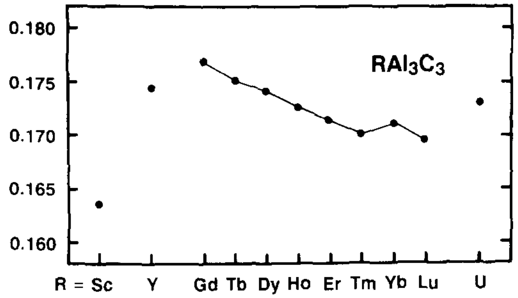

Fig. 2. Cell volumes of $YbAl_3C_3$ and UAl_3C_3 together with those of other $ScAl_3C_3$-type carbides reported earlier [12].

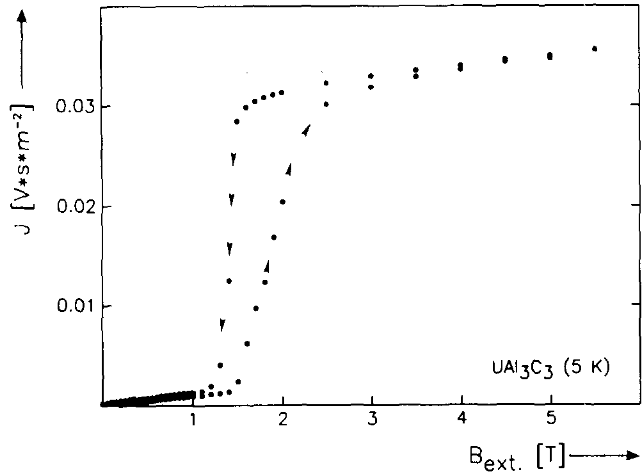

Fig. 3. Hysteresis curve of UAl_3C_3 at a temperature of 5 K.

by measuring the magnetization J *vs.* the magnetic field B at a temperature of 5 K (Fig. 3). The critical field is at about 1.5 T. Up to the highest obtainable magnetic field of 5.5 T the compound shows no magnetic saturation. Nevertheless, we have calculated the magnetic moment per uranium atom from that "saturation" magnetization; it amounts to $\mu_s \geqslant 0.27\ \mu_B$. This value is much smaller than the effective magnetic moment μ_{exp} determined from the slope of the $1/\chi$ *vs.* T plot. Possibly another metamagnetic step occurs at higher field strengths (multiple step metamagnetism, "devil staircase").

Electrical conductivity measurements of several samples of $YbAl_3C_3$ were made with an a.c. four-probe technique in a temperature range from 4 to about 400 K. Irregularly shaped pieces with dimensions of about $0.5 \times 0.5 \times 0.5$ mm^3 were contacted with copper filaments using a silver epoxy cement. Because of the uncertainties in estimating the size of the contacting areas, the absolute values of the electrical conductivities are estimated to be correct only within a factor of 2. The relative values at different temperatures are much more reliable (Fig. 4). The resistivity of $YbAl_3C_3$ decreases with increasing

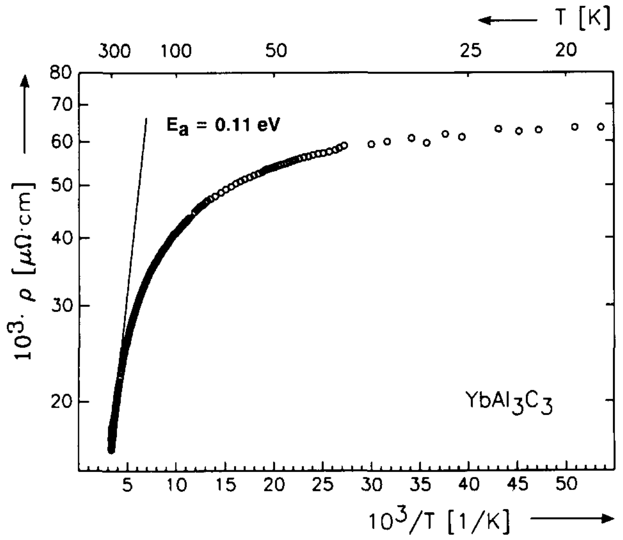

Fig. 4. Electrical resistivity of semiconducting $YbAl_3C_3$. The activation energy E_a was calculated from the steepest portion of the lnρ *vs.* $1/T$ plot.

temperatures, as is typical for semiconductors; however, the linear lnρ *vs.* $1/T$ behaviour to be expected for high temperatures was not reached. The activation energy corresponding to the steepest portion of the plot was calculated from the equation $\rho = \rho_0 \exp(E_a/2kT)$. The value $E_a \geqslant 0.11$ eV thus obtained is small and the intrinsic bond gap may be much larger. Semiconductivity was also observed for the carbides $LnRhC_2$(Ln≡La, Ce) [19], $Sc_5Re_2C_7$ [20] and $ScT_{1-x}C_2$ (T≡Fe, Co, Ni) [21], while the carbides $Y_8Rh_5C_{12}$ [22] and $LnRhC_2$ (Ln≡Pr, Nd) [19] show metallic behaviour.

4. Structure refinement of UAl_3C_3

The single crystals of UAl_3C_3 used for the structure refinement had been grown in an arc-melting furnace as described above. They were isolated from the crushed buttons and sealed into evacuated, thin-walled silica tubes to prevent hydrolysis.

The crystals were investigated in Buerger precession and Weissenberg cameras to establish their suitability for intensity data collection. The isotypy of UAl_3C_3 with $ScAl_3C_3$ was already recognized from the Guinier powder patterns. The structure refinement confirmed the space group *P*6₃/*mmc* (No. 194). Intensity data of a crystal with dimensions 25×100×200 μm^3 were recorded on a four-circle diffractometer with graphite-monochromated Mo Kα radiation, a scintillation counter and a pulse height discriminator. Background counts were taken at both ends of each $\theta/2\theta$ scan. An empirical absorption correction was made from ψ scan data. The ratio of the highest to the lowest transmission was 6.3:1. A further absorption correction was made with the programme DIFABS [23]. The theoretical density of UAl_3C_3 is $\rho_c = 6.82$ g cm^{-1}. A total of 4816 reflections was recorded in one half of the reciprocal sphere. After averaging the data and omitting those with $I < 3\sigma(I_0)$, 231 independent structure factors were obtained. The inner residual was $R_i = 0.025$.

The starting atomic parameters were taken from the previous structure determination of $ScAl_3C_3$ [12]. The structure was refined by full-matrix least-squares calculations with atomic scattering factors [24] corrected for anomalous dispersion [25]. The weighting scheme reflected the counting statistics. A parameter for an isotropic secondary extinction correction was refined and applied to the calculated structure factors. To check for deviations from the ideal composition, one series of least-squares cycles was calculated where all occupancy parameters (with fixed scale factor) were allowed to vary together with the thermal parameters. The results (in percentages with standard deviations in the position of the least significant digit in parentheses) were as follows: U, 100.0(4); Al1, 99(2); Al2, 99(3); C1, 93(6); C2, 106(10). Thus no significant deviations from the full occupancies were observed and in the final least-squares cycles the ideal occupancies were assumed. The refinement with anisotropic thermal parameters resulted in a thermal parameter B_{33} of the Al2 atom which was 19 times larger than its B_{11} parameter, We therefore preferred to refine this atom with a split position in 4f ($\frac{1}{3}$, $\frac{2}{3}$, z) rather than in 2d ($\frac{1}{3}$, $\frac{2}{3}$, $\frac{3}{4}$). In the final refinements the U and the Al1 atoms were allowed ellipsoidal thermal parameters; the other atoms had isotropic ones. A final difference Fourier synthesis gave no indication for the occupancy of additional atomic sites. The final conventional and weighted residuals are $R = 0.039$ and $R_w = 0.058$ for 231 structure factors and 12 variable parameters. The atomic parameters and the interatomic distances are given in Tables 2 and 3 respectively. A projection of the crystal structure is shown in Fig. 5. Listings of the anisotropic thermal parameters and the structure factors are available from the authors.

TABLE 2

Atomic parameters of UAl_3C_3[a]

Atom	$P6_3/mmc$	x	y	z	B[a]
U	2a	0	0	0	0.283(7)
Al1	4f	$\frac{1}{3}$	$\frac{2}{3}$	0.1346(4)	0.40(6)
Al2	4f	$\frac{1}{3}$	$\frac{2}{3}$	0.7406(7)	0.3(1)
C1	4f	$\frac{1}{3}$	$\frac{2}{3}$	0.594(1)	0.8(3)
C2	2c	$\frac{1}{3}$	$\frac{2}{3}$	$\frac{1}{4}$	0.6(3)

[a]Standard deviations in the positions of the least significant digits are given in parentheses. The last column contains the isotropic thermal parameters of the Al2 and C atoms and the equivalent isotopic thermal parameters B ($\times 100$, nm^2) of the U and Al1 atoms. The positions of the Al2 atoms are occupied to only 50%.

TABLE 3

Interatomic distances (pm) in UAl_3C_3[a]

U:	6	C1	254.8	Al1:	1	C2	200.7	C1:	3	Al1	208.1
	6	Al1	305.1		3	C1	208.1		3	U	254.8
	6	U	338.9		3	Al2	268.8		1	Al2	255.2
					3	Al2	292.2		1	Al2	287.9
					3	U	305.1				
								C2:	6	Al2	196.3
				Al2:	(1	Al2	32.7)		2	Al1	200.7
					3	C2	196.3				
					1	C1	255.2				
					1	C1	287.9				
					3	Al1	268.8				
					3	Al1	292.2				

[a] All distances shorter than 500 pm (U–U), 390 pm (U–Al, U–C, Al–C) and 330 pm (Al–Al, C–C) are listed. Standard deviations are all equal or less than 0.5 pm (metal–metal) and 2 pm (metal–carbon). The Al2 positions are occupied to only 50%.

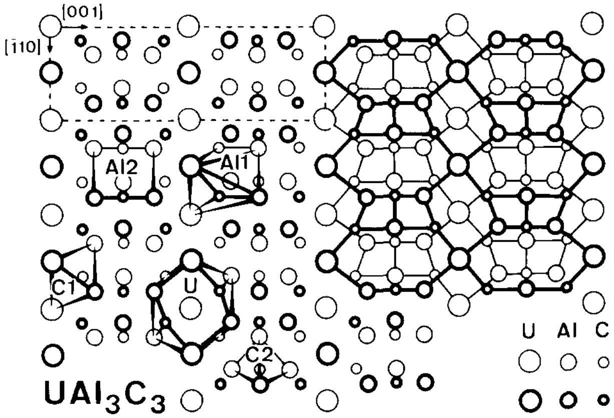

Fig. 5. Crystal structure and coordination polyhedra of the $ScAl_3C_3$-type structure of UAl_3C_3. The structure is projected on the (110) plane. The atoms are situated on mirror planes at two heights of the projection direction which are indicated by thin and thick lines. The Al2 atoms were refined with split positions. They are shown here in the average position, which may be the true position at high temperature.

5. Discussion

Tsokol' *et al.* [12] have determined the structure of $ScAl_3C_3$ and prepared the isotypic series RAl_3C_3 (R≡Y, Gd–Tm, Lu). $YbAl_3C_3$ is reported here for the first time. We obtained this compound by arc melting only together with some second- and/or third-phase products. It was prepared, however, in a pure form from the lithium flux. To our knowledge this is the first time that a lithium flux has been used for the preparation of a carbide. It has, however, been used before to synthesize well-crystallized borides [26].

The structure refinement of UAl_3C_3 essentially resulted in the same structure as that found before for $ScAl_3C_3$ [12]. The U atoms have (distorted) octahedral carbon coordination. The Al1 atoms have four C atom neighbours at an average distance of 206.3 pm forming a tetrahedron. In the structure determination of the prototype $ScAl_3C_3$ the Al2 atoms were found in a trigonal planar carbon coordination (with Al2–C distances of 194 pm) augmented with two additional C atoms (at 272 pm), thus forming a stretched trigonal bipyramidal environment. With $B = 2.9 \pm 0.2$ Å^2 the thermal parameter of this atom was found to be rather high [12]. In UAl_3C_3 we have refined this atom with a split position. In this way the Al2 atoms obtain a distorted tetrahedral carbon coordination with three C atom neighbours at 196 pm and one at 255 pm. The average Al2–C distance of 211.0 pm is only somewhat greater than the average tetrahedral Al1–C distance of 206.3 pm, as could be expected for a distorted coordination. Some further support for our preference to refine the Al2 atoms in the structure of UAl_3C_3 with a split position comes from a comparison with the structure of Al_4C_3 [2]. There both sites for the Al atoms have tetrahedral carbon coordination with average Al–C distances of 201 and 210 pm. It seems possible that at high temperature the Al2 atoms of UAl_3C_3 occupy the trigonal bipyramidal site, and upon cooling, the structure lowers its symmetry and the Al2 atoms order in a tetrahedral site. Such a displacive phase transition usually results in twin domains [27], but the *average* structure of the two domains would still have the higher symmetry space group. We therefore made no attempt to refine the structure in a space group of lower symmetry.

In addition to the C atoms, the coordination polyhedra of the metal atoms in UAl_3C_3 also contain many metal atoms of both kinds. The shortest Al–Al distances of 269 pm in these polyhedra are considerably shorter than the Al–Al distances of 286 pm in c.c.p. elemental aluminium. Nevertheless, it seems unlikely that these distances correspond to bonding interactions, considering that the shortest Al–Al distances in the transparent, light yellow (more or less ionic) carbide Al_4C_3 [2] are of about the same length (271 pm). This is also supported by the semiconducting behaviour found for the isotypic compound $YbAl_3C_3$ in the present investigation. Thus these compounds may be formulated as $A^{3+}(Al^{3+})_3(C^{4-})_3$, where the superscripts indicate oxidation numbers (formal charges). The metal–carbon interactions may have considerable covalent character, but there is little or no metal–metal bonding.

The carbon atoms of UAl_3C_3 are situated on two different crystallographic sites. Two-thirds of them occupy octahedral voids formed by three Sc atoms at one side and three Al atoms at the other side. The remaining third of the C atoms occupy trigonal bipyramidal voids of Al atoms in the structure as refined for $ScAl_3C_3$ [12]. In our refinement of UAl_3C_3 with split Al2 positions these C atoms obtain a distorted bipyramidal aluminium coordination. In the closely related structure of Al_4C_3 [2] the C atoms occupy octahedral and tetrahedral voids in the ratio of 2:1.

The Sc and Al atoms in the structure of $ScAl_3C_3$ form two-dimensionally infinite close-packed arrays which are stacked along the *c* axis with the

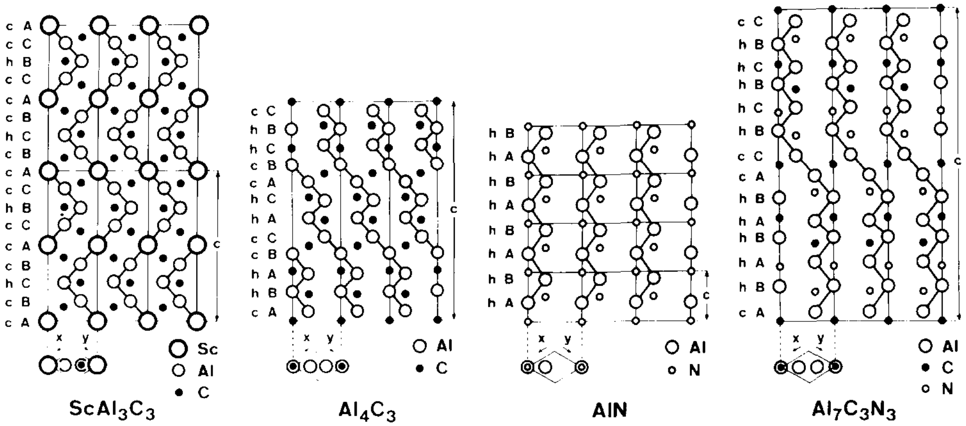

Fig. 6. The $ScAl_3C_3$-type structure as compared to the structure of Al_4C_3, AlN and $Al_7C_3N_3$. The structure are represented by cuts along the (110) plane of the hexagonal cells. The metal atoms form close-packed layers which are stacked with the indicated stacking sequences.

TABLE 4

Stacking sequences of the close-packed metal atoms in the Jagodzinski–Wykoff and Zhdanov notations in several structures related to the $ScAl_3C_3$-type structure

Formula	Jagodzinski–Wykoff	Zhdanov	Reference
$ScAl_3C_3$	$(hccc)_2$	$(4)_2$	[12]
Al_4C_3	$(hhcc)_3$	$(13)_3$	[2]
AlN	$(h)_2$	$(1)_2$	[28]
$Al_7C_3N_3$	$(hhhhhcc)_2$	$(11113)_2$	[29]
Al_5C_3N	$(hhhcc)_2$	$(113)_2$	[30, 31]
$Al_6C_3N_2$	$(hhhhcc)_3$	$(1113)_3$	[31]
$Al_8C_3N_4$	$(hhhhhhcc)_3$	$(111113)_3$	[31]

stacking sequence ABCBACBC. Using the Jagodzinski–Wykoff or the Zhdanov notations, these stacking sequences are represented by $(hccc)_2$ or 44 respectively. Close-packed aluminium layers also occur in the structures of Al_4C_3, AlN [28] and $Al_7C_3N_3$ [29]. This is shown in Fig. 6. In Table 4 the stacking sequences of these structures are described together with those of other closely related aluminium carbonitride structures with even more complicated stacking sequences.

Acknowledgments

We appreciated the helpful discussions with Dr. D. Kaczorowsky about the magnetic properties of UAl_3C_3 and we thank Mrs. U. Rodewald and Dr. M. H. Möller for the collection of the single-crystal diffractometer data. Mr. K. Wagner characterized our samples in the scanning electron microscope. We are also indebted to Mrs. J. Nowitzki and Mr. H. Rabeneck for the determination of the magnetic susceptibilities and for the analyses of our hydrolyses products. Dr. G. Höfer (Heraeus Quarzschmelze) is thanked for generous gifts of silica tubes. This work was supported by the Fonds der Chemischen Industrie and the Deutsche Forschungsgemeinschaft. Last but not least we acknowledge the Fonds der Chemischen Industrie for a stipend to R.P.

References

1 H. Moissan, *C.R. Acad. Sci. (Paris) 119* (1894) 935.
2 M. v. Stackelberg and E. Schnorrenberg, *Z. Phys. Chem. B, 27* (1934) 37.
3 W. Jeitschko, H. Nowotny and F. Benesovsky, *Monatsh. Chem.*, *94* (1963) 672.
4 W. Jeitschko, H. Nowotny and F. Benesovsky, *Monatsh. Chem.*, *94* (1963) 247.
5 S. Rosen and P. G. Sprang, *Adv. X-ray Anal.*, *8* (1965) 91.
6 E. Reiffenstein, H. Nowotny and F. Benesovsky, *Monatsh. Chem.*, *97* (1966) 499.
7 S. I. Mikhalenko, Yu. B. Kuz'ma, V. E. Popov, V. N. Gurin and A. P. Nechitailov, *Izv. Akad. Nauk SSSR, Neorg. Mater.*, *15* (1979) 1948.
8 J. C. Schuster and H. Nowotny, *Z. Metallk.*, *71* (1980) 341.
9 S. Sridharan, H. Nowotny and S. F. Wayne, *Monatsh. Chem.*, *114* (1983) 127.
10 C. Brisi and F. Abbattista, *Ann. Chim. Rome*, *51* (1961) 452.
11 V. Cirilli and C. Brisi, *Atti Accad. Sci. Tor.*, *94* (1959) 424.
12 A. O. Tsokol', O. I. Bodak, E. P. Marusin and M. G. Baivel'man, *Sov. Phys.—Crystallogr.*, *31* (1986) 467.
13 K. Yvon, W. Jeitschko and E. Parthé, *J. Appl. Crystallogr.*, *10* (1977) 73.
14 J. Bauer and H. Bienvenu, *C.R. Acad. Sci. C, 290* (1980) 387.
15 R. Pöttgen and W. Jeitschko, *Inorg. Chem.*, *30* (1991) 427.
16 F. H. Spedding, K. Gschneidner Jr. and A. H. Daane, *J. Am. Chem. Soc.*, *80* (1958) 4499.
17 B. Hájek, P. Karen and V. Brožek, *J. Less-Common Met.*, *96* (1984) 35.
18 W. Jeitschko and M. Reehuis, *J. Phys. Chem. Solids.*, *48* (1987) 667.
19 R.-D. Hoffmann, W. Jeitschko and L. Boonk, *Chem. Mater.*, *1* (1989) 580.
20 R. Pöttgen and W. Jeitschko, *Z. Naturforsch.*, *47b* (1992) 358.
21 R. Pöttgen, W. Jeitschko, U. Wortmann and M. E. Danebrock, *J. Mater. Chem.*, in the press.
22 R.-D. Hoffmann, W. Jeitschko, M. Reehuis and S. Lee, *Inorg. Chem.*, *28* (1989) 934.
23 N. Waker and D. Stuart, *Acta Crystallogr. A*, *39* (1983) 158.
24 D. T. Cromer and J. B. Mann, *Acta Crystallogr. A*, *24* (1968) 321.
25 D. T. Cromer and D. Liberman, *J. Chem. Phys.*, *53* (1970) 1891.
26 W. Jung and F. Diessenbacher, *Z. anorg. allg. Chem.*, *594* (1991) 57.
27 H. Wondratschek and W. Jeitschko, *Acta Crystallogr. A*, *32* (1976) 664.
28 G. A. Jeffrey and G. S. Parry, *J. Chem. Phys.*, *23* (1955) 406.
29 G. A. Jeffrey and V. Y. Wu, *Acta Crystallogr.*, *16* (1963) 559.
30 M. v. Stackelberg and K. F. Spiess, *Z. Phys. Chem. A, 175* (1935) 140.
31 G. A. Jeffrey and V. Y. Wu, *Acta Crystallogr.*, *20* (1966) 538.